

Yamashita, K., Totani, K., Ohkura, T., Takasaki, S., Goldstein, I. J., & Kobata, A. (1987) *J. Biol. Chem.* 262, 1602-1607.
Yamashita, K., Koide, N., Endo, T., Iwaki, Y., & Kobata, A. (1989a) *J. Biol. Chem.* 264, 2415-2423.
Yamashita, K., Totani, K., Iwaki, Y., Takamizawa, I., Ta-

teishi, N., Higashi, T., Sakamoto, Y., & Kobata, A. (1989b) *J. Biochem. (Tokyo)* 105, 728-735.
Yazawa, S., Furukawa, K., & Kochibe, N. (1984) *J. Biochem. (Tokyo)* 96, 1737-1742.
Yoshima, H., Matsumoto, A., Mizuochi, T., Kawasaki, T., & Kobata, A. (1981) *J. Biol. Chem.* 256, 8476-8484.

Low-Resolution Structure of the Tetrameric Phenylalanyl-tRNA Synthetase from *Escherichia coli*. A Neutron Small-Angle Scattering Study of Hybrids Composed of Protonated and Deuterated Protomers

Philippe Dessen,^{*,†} Arnaud Ducruix,[§] Roland P. May,^{||} and Sylvain Blanquet[‡]

Appendix: Considerations on Stuhmann Plots of Particles with Two Constituents of Different Scattering Length Density

Roland P. May,^{||} Philippe Dessen,^{*,†} and Arnaud Ducruix[§]

Laboratoire de Biochimie, Ecole Polytechnique, URA 240 du Centre National de la Recherche Scientifique, 91128 Palaiseau Cedex, France, Institut de Chimie des Substances Naturelles, LP 2301 du Centre National de la Recherche Scientifique, 91198 Gif sur Yvette Cedex, France, and Institut Max von Laue-Paul Langevin, BP156X, 38042 Grenoble Cedex, France

Received June 21, 1989; Revised Manuscript Received October 26, 1989

ABSTRACT: *Escherichia coli* phenylalanyl-tRNA synthetase is a tetrameric protein composed of two types of protomers. In order to resolve the subunit organization, neutron small-angle scattering experiments have been performed in different contrasts with all types of isotope hybrids that could be obtained by reconstituting the $\alpha_2\beta_2$ enzyme from the protonated and deuterated forms of the α and β subunits. Experiments have been also made with the isolated α promoter. A model for the $\alpha_2\beta_2$ tetramer is deduced where the two α promoters are elongated ellipsoids ($45 \times 45 \times 160 \text{ \AA}^3$) lying side by side with an angle of about 40° between their long axes and where the two β subunits are also elongated ellipsoids ($31 \times 31 \times 130 \text{ \AA}^3$) with an angle of 30° between their axes. This model was obtained by assuming that the two pairs of subunits are in contact in an orthogonal manner and by taking advantage of the measured distance between the centers of mass of the α_2 and β_2 pairs ($d = 23 \pm 2 \text{ \AA}$).

Aminoacyl-tRNA synthetases catalyze the esterification of amino acids to tRNAs (Schimmel et al., 1979). For the same mode of reaction, this family of enzymes displays a variety of quaternary structures (monomeric, dimeric, and tetrameric). Among the 20 *Escherichia coli* aminoacyl-tRNA synthetases, only two (phenylalanyl- and glycyl-tRNA synthetases) form $\alpha_2\beta_2$ structures.

It was shown (Ducruix et al., 1983) that it is possible to reversibly dissociate the phenylalanyl-tRNA synthetase enzyme subunits in the presence of sodium thiocyanate. Dissociated α and β subunits can be isolated by gel filtration, neither of the subunits showing any significant enzymatic activity. Upon mixing of stoichiometric amounts of each subunit, a fully active $\alpha_2\beta_2$ enzyme is recovered.

The two genes pheS and pheT, coding for the two subunits of phenylalanyl-tRNA synthetase, were cloned in plasmid pBR322 (Plumbridge et al., 1980). The recombinant plasmid pB1 is responsible for the overproduction of the enzyme by a factor of more than 100 (Fayat et al., 1983a).

Because of the overproduction and the dissociation properties of the enzyme, it became possible to study the structure of the tetrameric enzyme at low resolution by combining the small-angle neutron scattering technique and specific deuteration of the promoters. Since neutron scattering offers the unique advantage that the scattering density of the solvent can be adjusted by varying the percentage of $^2\text{H}_2\text{O}$ in the solvent (Jacrot, 1976), we expected to measure the structural parameters of the enzyme by triangulation as shown for RNA polymerase (Stöckel et al., 1979, 1980a,b) or for methionyl-tRNA synthetase (Dessen et al., 1983a,b).

A study of the protonated form of the enzyme and its binding to tRNA^{Phe} has already been published (Dessen et al., 1983a,b). It showed that the radius of gyration is independent of the presence of MgCl_2 and that there is no detectable conformational change upon tRNA^{Phe} binding. It also allowed us to determine the enzyme molecular mass ratio, which was confirmed by the enzyme sequence, as deduced from genetic studies (Fayat et al., 1983b; Mechulam et al., 1985).

MATERIALS AND METHODS

Bacterial Strains and Growth Conditions. *Escherichia coli* strain IBPC 1671 carrying plasmid DNA pB1 (Plumbridge et al., 1980) was grown at 30°C in glucose minimal medium

* Address correspondence to this author.

† Laboratoire de Biochimie, Ecole Polytechnique, URA 240 du CNRS.

§ Institut de Chimie des Substances Naturelles, LP 2301 du CNRS.

|| Institut Max von Laue-Paul Langevin.

(M9) supplemented with the required amino acids (Arg, His, Pro) at 100 $\mu\text{g}/\text{mL}$, thiamin (0.5 $\mu\text{g}/\text{mL}$), and two antibiotics (10 $\text{mg}/\mu\text{L}$ tetracycline and 25 $\text{mg}/\mu\text{L}$ ampicillin). A 5-mL M9 culture was inoculated with a single colony freshly isolated from an M9 plate. The 5-mL culture was composed of 0.2 mL of protonated 40-fold-concentrated M9 medium and 4.8 mL of $^2\text{H}_2\text{O}$ (99.9% purity). In all cases, the required amino acids and the carbon source were in the protonated form. In these conditions, the lag before exponential growth is at least twice as long in the deuterated culture as in the protonated one (24 and 48 h, respectively). These 5-mL cultures were used at stationary phase to inoculate a 50-mL culture (H_2O or 96% $^2\text{H}_2\text{O}$), which was then used to inoculate a 1-L culture (H_2O or 96% $^2\text{H}_2\text{O}$). At saturation of the growth medium, roughly 3 g wet weight of cells was harvested from 1 L of culture. Cells were centrifuged for 1 h at 4300g, resuspended in M9 medium, and kept frozen at -20°C .

Deuteration Measurement. The deuteration medium was rotoevaporated and Millipore filtered (0.25 μm) in order to be reused several times. The level of $^2\text{H}_2\text{O}$ content in the cell culture was carefully monitored by ^1H NMR spectroscopy. It showed 95% at the end of the first culture and a 2% decrease after each further culture cycle. Cells harvested from three successive cultures were pooled before enzyme extraction. One culture was grown at a final percentage of 78% $^2\text{H}_2\text{O}$ in order to isolate deuterated α subunits.

Purification of Phenylalanyl-tRNA Synthetase. Protonated and deuterated phenylalanyl-tRNA synthetases were purified according to Ducruix et al. (1983). No differences in purification yields were observed.

Subunit Isolation and Hybrid Formation. Protonated and deuterated homogeneous enzymes were applied in parallel on two identical (2.2 \times 90 cm) Ultrogel AcA34 columns equilibrated with 100 mM phosphate (K^+), pH 7.0, 10 mM 2-mercaptoethanol, and 500 mM NaSCN, as described (Ducruix et al., 1983). α and β subunits migrated as protomers and not as dimers. In the case of protonated phenylalanyl-tRNA synthetase, little residual enzymatic activity could be measured in a few fractions eluted from the column, at the overlap of the α and β peaks. In the case of the deuterated enzyme, no activity could be detected between the two peaks.

Fractions of the elution profiles without activity were cross-pooled ($\alpha_{\text{H}} + \beta_{\text{D}}$, $\alpha_{\text{D}} + \beta_{\text{H}}$) and extensively dialyzed against 20 mM imidazole hydrochloride, pH 7.0, 10 mM 2-mercaptoethanol, 150 mM KCl, and 0.1 mM EDTA. Both hybrids ($\alpha_{\text{H}_2}\beta_{\text{D}_2}$, $\alpha_{\text{D}_2}\beta_{\text{H}_2}$) were further purified on a (2.2 \times 90 cm) Sephadex G-200 column equilibrated in the same buffer. The reconstituted hybrids were indistinguishable from the native enzyme according to both nondenaturing PAGE and SDS-PAGE analysis and according to measurements of the rates of isotopic [^{32}P]PP_i-ATP exchange and tRNA^{Phe} aminoacylation (Ducruix et al., 1983).

Neutron Scattering Experiments. Small-angle neutron scattering experiments were performed on the D11 camera (Ibel, 1976) at the Institut Laue-Langevin, Grenoble, France. Samples were exposed to the neutron beam in Hellma quartz cells, according to Dessen et al. (1978). Scattering curves were observed with a wavelength λ of 10.0 Å in the range $0.0012 \text{ \AA}^{-1} < s < 0.0075 \text{ \AA}^{-1}$ [$s = 2(\sin \theta)/\lambda$], where 2θ is the full scattering angle, with a sample-to-detector distance of 4.84 m and a collimation of 3.3 m. All experiments were performed at room temperature.

For each contrast, four samples were prepared: fully protonated ($\alpha_{\text{H}_2}\beta_{\text{H}_2}$), fully deuterated ($\alpha_{\text{D}_2}\beta_{\text{D}_2}$), and the two hybrids ($\alpha_{\text{H}_2}\beta_{\text{D}_2}$ and $\alpha_{\text{D}_2}\beta_{\text{H}_2}$). Samples were dialyzed three times

against 20 mM phosphate (K^+), pH 7.0, containing 10 mM 2-mercaptoethanol, 0.1 mM EDTA, and 150 mM KCl, at various $^2\text{H}_2\text{O}/\text{H}_2\text{O}$ ratios. The α subunits (α_{H} and α_{D}) were prepared in the same way.

The intensity data, $I(s)$, were analyzed according to the Guinier (1955) approximation in the low s limit:

$$\ln I(s) = \ln I(0) - (4/3)\pi^2 R_G^2 s^2 \quad (1)$$

The $I(0)$ and R_G variations were analyzed as a function of $^2\text{H}_2\text{O}$ as follows: for each of the four tetramer forms ($\alpha_{\text{H}_2}\beta_{\text{H}_2}$, $\alpha_{\text{H}_2}\beta_{\text{D}_2}$, $\alpha_{\text{D}_2}\beta_{\text{H}_2}$, and $\alpha_{\text{D}_2}\beta_{\text{D}_2}$), the forward scattering intensity can be written as

$$I(0) = 4C_i(A_{1\delta} + A_{2\delta})^2 \quad (2)$$

where C_i is the molar concentration of the tetramer and $A_{1\delta}$ and $A_{2\delta}$ correspond to the scattering amplitude contributions of each subunit (α and β).

The analysis of the variation of R_G^2 as a function of the $^2\text{H}_2\text{O}$ content can be interpreted with the Stuhmann (1974) equation:

$$R_G^2 = R_C^2 + \alpha/\bar{\rho} - \beta/\bar{\rho}^2 \quad (3)$$

where R_C corresponds to the radius of gyration at infinite contrast, $\bar{\rho}$ corresponds to the excess scattering length density, and the parameters α and β relate to the nonhomogeneous scattering density of the particle (see appendix for a more precise definition).

The angular region used in the analysis corresponds to $s < 0.0051 \text{ \AA}^{-1}$ with measured $R_G = 48 \text{ \AA}$, so that $2\pi s R_G < 1.6$ (Guinier, 1955). A linear least-squares fit of the data in this range for each scattering curve yields $I(0)$ and R_G^2 values with associated standard values, which were interpreted by using eqs 1 and 2.

For enzyme concentration measurements, the optical extinction coefficient of phenylalanyl-tRNA synthetase was taken equal to $0.75 \pm 0.1 \text{ cm}^2\text{-mg}^{-1}$ at 280 nm (Fayat et al., 1974).

RESULTS

The use of contrast variation in neutron scattering has been extensively described [e.g., Koch et al. (1979) and Timmins et al. (1988)]. In this context, experiments with the $\alpha_2\beta_2$ *E. coli* phenylalanyl-tRNA synthetase were carried to record data on both sides of the match point, the buffer scattering density that matches the average scattering density of the particles. For each $\alpha_2\beta_2$ tetramer hybrid or nonhybrid, a series of measurements were performed (with exposure times of 1–6 h, depending on the proximity of the contrast to the match point) in buffers containing increasing quantities of $^2\text{H}_2\text{O}$.

Figure 1 shows typical Guinier plots ($\ln I$ versus s^2) with the four enzyme species, in 0% and 98% $^2\text{H}_2\text{O}$, respectively. Experiments with deuterated enzyme in a deuterated buffer showed a slight tendency to aggregation. Table I presents the amplitude values and the radii of gyration extrapolated from Guinier plots in H_2O .

Amplitude Analysis. Figure 2 summarizes amplitude variations of all species as a function of the $^2\text{H}_2\text{O}$ content in the buffer. For the protonated $\alpha_{\text{H}_2}\beta_{\text{H}_2}$ enzyme, it is possible to derive a straight line from the experimental points on both sides of the match point. On the contrary, for the fully deuterated tetramer $\alpha_{\text{D}_2}\beta_{\text{D}_2}$, the $^2\text{H}_2\text{O}$ concentration value at the match point (90%) prevented collection of negative amplitude values.

As expected from the contrast variation theory (Koch et al., 1979), the monodisperse solutions $\alpha_{\text{H}_2}\beta_{\text{H}_2}$, $\alpha_{\text{H}_2}\beta_{\text{D}_2}$, $\alpha_{\text{D}_2}\beta_{\text{H}_2}$, and $\alpha_{\text{D}_2}\beta_{\text{D}_2}$ give straight lines in this plot (Stuhmann, 1974). Since the exchange of the labile hydrogens in the α and β subunits

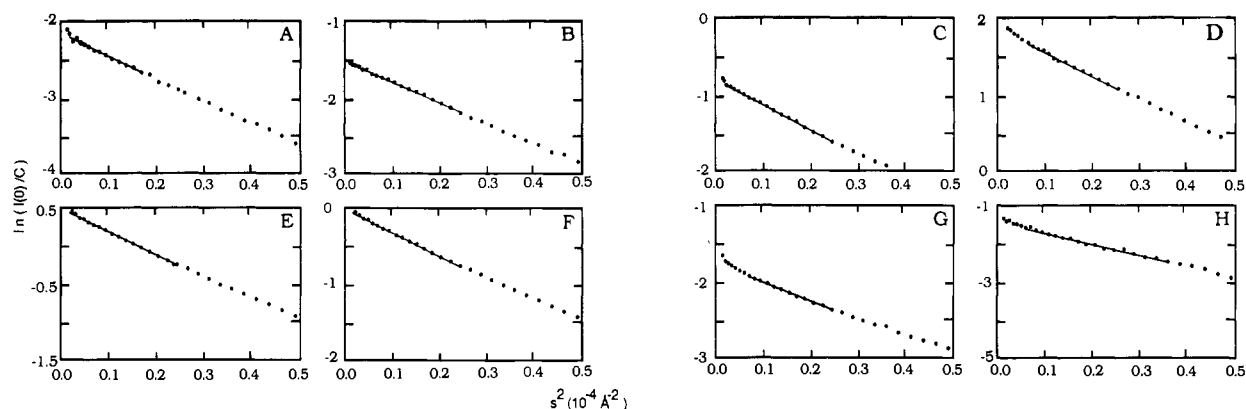


FIGURE 1: Guinier plots of various deuterated forms of phenylalanyl-tRNA synthetase: The logarithms of scattering intensities $[I(0)/c]$ are plotted versus s^2 . Guinier approximations of the scattering data are indicated by straight lines. Upper panels correspond to experiments in H_2O : (A) $\alpha_{H_2}\beta_{H_2}$, 6.86 mg/mL; (B) $\alpha_{H_2}\beta_{D_2}$, 5.98 mg/mL; (C) $\alpha_{D_2}\beta_{H_2}$, 6.85 mg/mL; (D) $\alpha_{D_2}\beta_{D_2}$, 5.78 mg/mL. Lower panels correspond to experiments in high concentrations of 2H_2O : (E) $\alpha_{H_2}\beta_{H_2}$, 6.63 mg/mL (98% 2H_2O); (F) $\alpha_{H_2}\beta_{D_2}$, 4.11 mg/mL (98% 2H_2O); (G) $\alpha_{D_2}\beta_{H_2}$, 4.47 mg/mL (98% 2H_2O); (H) $\alpha_{D_2}\beta_{D_2}$, 4.97 mg/mL (80% 2H_2O).

Table I: Experimental Neutron Scattering Amplitudes and Radii of Gyration of the Samples in H_2O Scattering Buffer (0% 2H_2O Content) for the Various Tetrameric Species and for α_H and α_D Subunits^a

	$\alpha_{H_2}\beta_{H_2}$	$\alpha_{H_2}\beta_{D_2}$	$\alpha_{D_2}\beta_{H_2}$	$\alpha_{D_2}\beta_{D_2}$	α_H	α_D
scattering amplitudes in H_2O (relative to H_2O scattering)	0.512 ± 0.031	0.715 ± 0.045	1.024 ± 0.066	1.227 ± 0.080	0.325 ± 0.089	0.649 ± 0.054
radius of gyration (\AA)	48.0 ± 0.6	46.3 ± 0.5	50.5 ± 0.4	49.7 ± 0.4	38.4 ± 1.5	38.4 ± 0.5
match point in units of $[^2H_2O]/[H_2O + ^2H_2O]$	0.374	0.521	0.747	0.894	0.375	0.828

^a The indices H and D stand for the deuteration state of the subunits: H means protonated; D, deuterated.

Table II: Physical Parameters for Phenylalanyl-tRNA Synthetase from *Escherichia coli*

	α	β	$\alpha_2\beta_2$	
relative molecular mass (sequence), M_r	87 200	36 720	247 850	
partial specific volume, \bar{v} (cm ³ ·g ⁻¹)	0.76	0.76	0.76	
particle volume, V (Å ³) (assuming no hydration)	110 580	46 513	314 285	
hydrated particle volume, V (Å ³) [% w/w]	167 508 [39.3]	70 477 [39.3]	475 700 [41.0]	
percentage of exchangeable non-C bound hydrogens, γ	80	80	80	
	$\alpha_{H_2}\beta_{H_2}$	$\alpha_{H_2}\beta_{D_2}$	$\alpha_{D_2}\beta_{H_2}$	$\alpha_{D_2}\beta_{D_2}$
total scattering length of the molecule				
protonated, $\sum b_{H_2O}$ (10 ⁻¹² cm)	5621	8568	13 041	15 985
deuterated, $\sum b_{D_2O}$ (10 ⁻¹² cm)	9635	12 583	17 055	20 003
match point	0.403	0.564	0.807	0.968
scattering amplitude (10 ⁻⁹ cm)				
in 0% ² H ₂ O	7.412	10.359	14.832	17.779
in 100% ² H ₂ O	-10.961	-8.013	-3.540	-0.593

^a The dry volume V excludes the solvent; i.e., it is the volume occupied by the atoms in the particle. It is calculated from $V = M\bar{v}/N$. The \bar{v} value and the total scattering lengths $\sum b_{H_2O}$ and $\sum b_{D_2O}$ of the enzyme are calculated from the chemical composition (Ducruix et al., 1983; Fayat et al., 1983b; Mechulam et al., 1985) and the scattering data (Jacrot, 1976). γ is estimated from \bar{v} and from the 2H_2O proportion (38%) in which the scattering amplitude of the solvent matches that of the protonated form of the enzyme. The values concerning the deuterated enzyme take in account the auxotrophies of the strain for arginine, proline, and histidine and the level of deuteration in the culture (86.5%).

of the dimer can be assumed to be independent of the degree of deuteration, the lines corresponding to the different species were imposed as parallel. With this constraint, a linear regression on all points leads to (i) amplitudes at 0% 2H_2O for each species and (ii) a mean slope corresponding to the rate of exchange of the labile hydrogens. Deduced match points are reported in Table II.

The absolute value of $I(0)/c$ is related to the relative molecular mass of the protein, to its partial specific volume, and to the specific scattering length (Jacrot, 1976) calculated from the amino acid composition (May et al., 1983; Lederer et al., 1986; Mechulam et al., 1985). In H_2O buffer, $I(0)$ is nearly independent of the value of the partial specific volume (Zaccai et al., 1982). For the $\alpha_{H_2}\beta_{H_2}$ dimer, $I(0)/c$ gives a relative molecular mass of 240 000, in good agreement with $227\,000 \pm 20\,000$, the value previously determined by the same technique (Dessen et al., 1983a,b), and with 247 850, the value deduced from DNA sequence studies (Fayat et al., 1983b;

Mechulam et al., 1985). Table III shows the amino acid composition for each subunit of the $\alpha_2\beta_2$ phenylalanyl-tRNA synthetase (Fayat et al., 1983b; Mechulam et al., 1985). No important differences in composition are observed for the subunits in terms of scattering length. Moreover, the three amino acids (Arg, His, and Pro) corresponding to the auxotrophies of the host *E. coli* strain (Plumbridge et al., 1980) and supplied in protonated form in the culture medium are equally distributed between the subunits. The contributions of these amino acids to the scattering lengths in H_2O are 17.8% and 19.9% for the α and β subunits, respectively. These remarks imply that, for a given deuteration, the scattering densities of both subunits should remain the same.

In H_2O , the ratio of the experimental amplitudes $[I(0)/c]^{1/2}$ for the $\alpha_{D_2}\beta_{D_2}$ and $\alpha_{H_2}\beta_{H_2}$ species is 2.4. This is in reasonable agreement with the ratio of 2.6 that can be predicted from (i) the deuteration conditions in the cell cultures (a mean of $92\% \pm 2\%$ 2H_2O), (ii) the auxotrophies of the host strain, and (iii)

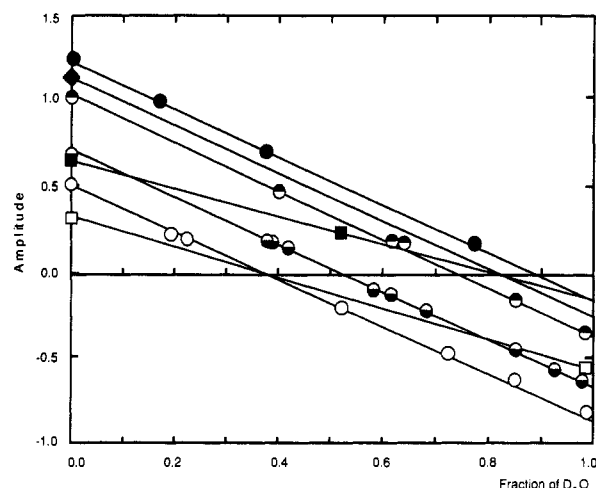


FIGURE 2: Neutron scattering amplitude $[I(0)/c]^{1/2}$ as function of solvent $^2\text{H}_2\text{O}$ concentration for the fully protonated $\alpha_{\text{H}_2}\beta_{\text{H}_2}$ (○), fully deuterated $\alpha_{\text{D}_2}\beta_{\text{D}_2}$ (●), 80% deuterated $\alpha_{\text{D}_2}\beta_{\text{D}_2}$ (◆), and the two mixed hybrid forms $\alpha_{\text{H}_2}\beta_{\text{D}_2}$ (◐) and $\alpha_{\text{D}_2}\beta_{\text{H}_2}$ (◑) of phenylalanyl-tRNA synthetase. Solutions are in 20 mM phosphate (K^+), pH 7.0, 10 mM 2-mercaptoethanol, 0.1 mM EDTA, and 150 mM KCl, containing enzymes at concentrations from 3.3 to 4.6 mg/mL and variable percentages of $^2\text{H}_2\text{O}$. Continuous lines correspond to an optimization of all the experimental data by global linear regression with the constraint of parallelism. All the points are distributed on straight lines within experimental errors. Data for the protonated (□) and 80% deuterated (■) α subunits are also shown. Experimental errors on amplitude values are of the order of 3%, smaller than the size of the symbols used in the figure.

Table III: Amino Acid Compositions of Phenylalanyl-tRNA Synthetase and Its Subunits^a

	α	β	$\alpha_2\beta_2$
Ala	69 (8.68)	29 (8.86)	196 (8.73)
Cys	13 (1.63)	1 (0.30)	28 (1.24)
Asp	52 (6.54)	19 (5.81)	142 (6.33)
Glu	65 (8.18)	24 (7.34)	178 (7.93)
Phe	19 (2.39)	20 (6.12)	78 (3.48)
Gly	64 (8.05)	22 (6.72)	172 (7.72)
His ^b	17 (2.14)	10 (3.05)	54 (2.41)
Ile	50 (6.29)	16 (4.89)	132 (5.88)
Lys	35 (4.40)	11 (3.37)	92 (4.10)
Leu	83 (10.44)	31 (9.48)	228 (10.16)
Met	14 (1.76)	10 (3.05)	48 (2.13)
Asn	32 (4.02)	15 (4.38)	94 (4.19)
Pro ^b	35 (4.40)	17 (5.20)	104 (4.63)
Gln	23 (2.89)	13 (3.97)	72 (3.20)
Arg ^b	54 (6.79)	24 (7.33)	156 (6.95)
Ser	32 (4.02)	14 (4.28)	92 (4.10)
Thr	37 (4.65)	22 (6.72)	118 (5.26)
Val	79 (9.93)	20 (6.11)	198 (8.82)
Trp	8 (1.00)	2 (0.61)	20 (0.89)
Tyr	14 (1.76)	7 (2.14)	42 (1.87)
total	795 (100)	327 (100)	2244 (100)

^a Deduced from the sequence (Fayat et al., 1983b; Mechulam et al., 1985). Note that the average composition differs in the two subunits, especially for cysteine and phenylalanine. All values in parentheses correspond to amino acid percentages. ^b Amino acids required for the cultures because of the auxotrophy.

the assumption that 80% of the labeled hydrogens have exchanged with the buffer. For the $\alpha_{\text{H}_2}\beta_{\text{D}_2}$ and $\alpha_{\text{D}_2}\beta_{\text{H}_2}$ isotope hybrids, ratio values of 1.4 and 2.0 with respect to the $\alpha_{\text{H}_2}\beta_{\text{H}_2}$ species are also in good agreement with the values obtained with the hypotheses mentioned above. With these conditions, the deuteration level of the tetramer can be estimated to be $86\% \pm 8\%$.

Isolated subunits were also studied. However, data could be obtained only for the large α subunit. The solution with the small β particles could not be deprived of sodium thio-

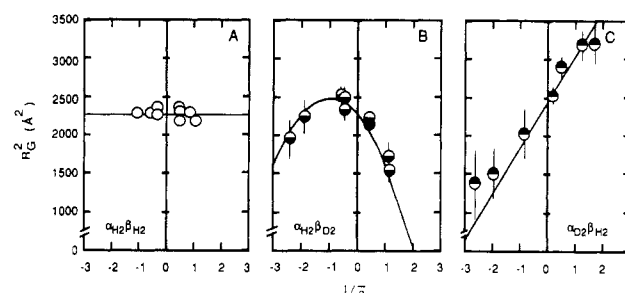


FIGURE 3: Square of the radii of gyration as function of the reciprocal contrast ($1/\bar{\rho}$) for the fully protonated $\alpha_{\text{H}_2}\beta_{\text{H}_2}$ (○) and the two mixed hybrid forms $\alpha_{\text{H}_2}\beta_{\text{D}_2}$ (◐) and $\alpha_{\text{D}_2}\beta_{\text{H}_2}$ (◑) of phenylalanyl-tRNA synthetase. Experimental conditions are the same as described in Figure 2.

cyanate without precipitation. For the protonated α subunit in solution, the extrapolated $[I(0)/c]^{1/2}$ value in H_2O leads to a relative molecular mass of $95\,000 \pm 10\,000$, in good agreement with the theoretical mass. It also implies that the isolated α promoter behaves as a monomer, even at a concentration of 6 mg/mL. For the protonated α subunit, two points (at 0% and 97.8% $^2\text{H}_2\text{O}$) were recorded, and the line through the points gives the same match point as for the protonated $\alpha_2\beta_2$ enzyme (Figure 2). For the deuterated α subunit, two points were recorded (0 and 55%), and the resulting line ($[I(0)]^{1/2}$ versus $^2\text{H}_2\text{O}$ content of the scattering buffer) indicates a match point identical with that of the deuterated $\alpha_2\beta_2$ enzyme from which the α subunit was prepared. The latter deuterated enzyme was prepared from a 78% $^2\text{H}_2\text{O}$ culture (see Materials and Methods). The match point of this deuterated $\alpha_{\text{D}_2}\beta_{\text{D}_2}$ enzyme was obtained from one scattering experiment in H_2O and by tracing a parallel to the other amplitude variations in Figure 2. Its value (83% $^2\text{H}_2\text{O}$) corresponds to a deuteration level of 73%. The identity between the match point of the enzyme and that of the α subunit implies that the scattering density is conserved upon dissociation.

Radius of Gyration Analysis. Koch and Stuhmann (1979) have shown that, for an inhomogeneous particle composed of two subunits of different scattering length densities, the distance d between the centers of the scattering mass corresponding to the two pseudodimers can be obtained from the β parameter in eq 3.

In Figure 3, the three data sets are represented as R_G^2 versus ($1/\bar{\rho}$) ("Stuhrmann plots") where the R_G values are derived from the Guinier plots at given $^2\text{H}_2\text{O}$ concentrations. Experimental errors are large near the match point, even with measuring times as long as 4–6 h. As expected, the homogeneous species $\alpha_{\text{H}_2}\beta_{\text{H}_2}$ and $\alpha_{\text{D}_2}\beta_{\text{D}_2}$ do not show significant variation of R_G^2 versus ($1/\bar{\rho}$). For the two hybrids, both plots are quite different and can be interpreted as parabolas, even if Figure 3C shows only one side on the parabola.

The experimental points of $\alpha_{\text{H}_2}\beta_{\text{D}_2}$ in Figure 3B are easily fitted with a quadratic curve according to Stuhmann (Koch et al., 1979) (eq 3). The value of R_C (the radius of gyration of the particle at infinite contrast) is 47.8 ± 0.5 Å. The α term, which is given by the slope at infinite contrast ($1/\bar{\rho} \rightarrow 0$), reflects essentially the scattering density of the outer part of the particle. A non-zero α term can be interpreted as a nonuniform radial distribution of the scattering density, whereas the β term (always positive) is related to the displacement of the scattering mass center with the contrast. A non-zero β term implies a curvature of the R_G^2 variation. In our case, the curve is shifted from the origin of $1/\bar{\rho}$. The negative value of α (-379 ± 45) is characteristic of a particle

in which the regions of highest scattering density are on average located closer to the center of the particle than the regions of lowest density. The value of β (245 ± 31) clearly indicates a separation between the centers of mass of the α_{H_2} and β_{D_2} dimers in the tetramer.

In the case of $\alpha_{D_2}\beta_{H_2}$, where the deuteration of the α subunits is involved, a similar parabolic curve with a positive slope (α term) at infinite contrast is expected. The slope in Figure 3C is positive. However, surprisingly, the experimental points appear as a straight line, within error. As developed in the appendix, this results from the unequal size of the two types of subunits (M_r of $2 \times 37K$ and $2 \times 87K$, respectively) and from the relative scattering density of the deuterated α subunit. Due to the deuteration, the scattering contribution of the α subunit is 2.4 times greater than that of the β subunit. As a consequence, the quadratic curve is shifted sufficiently far away from the origin of $1/\bar{\rho}$ to mask the major part of the curve and to make it apparently linear in the explored experimental domain. In terms of scattering intensity, the contribution of the deuterated α subunit in the $\alpha_{D_2}\beta_{H_2}$ complex at 0% 2H_2O is 31 times greater than that of the small protonated β subunit. Because of such an unbalanced contribution, the accuracy on the measured points and, consequently, on the extrapolated distance d (which could be calculated from the curvature in Figure 3C) leads to meaningless values. On the contrary, values for $\alpha_{H_2}\beta_{D_2}$ in Figure 3B are precise enough because of a ratio of 1 between the contribution of the scattering intensities of the α_H and β_D species.

According to the calculations in the appendix and taking in mind the assumptions of (i) identical exchange of labile hydrogens in the two subunits and (ii) uniform scattering density of each promoter, a value of $23 \pm 2 \text{ \AA}$ is deduced for the distance d between the centers of mass of the α_2 and β_2 pairs in the enzyme.

By considering the specific deuteration of the α and β subunits in the tetramer and the variation of contrast, in situ R_G values of the α_2 and β_2 dimers can be extrapolated from eqs A7 and A10 of the appendix. Values of $51 \pm 2 \text{ \AA}$ and $39 \pm 2 \text{ \AA}$ are deduced for R_{G,α_2} and R_{G,β_2} , the radii of gyration of the α_2 and β_2 pairs in the tetramer, respectively. The R_G values obtained at infinite contrast in the tetramer (extrapolation to the zero value of $1/\bar{\rho}$) are nearly identical for $\alpha_{H_2}\beta_{H_2}$, $\alpha_{H_2}\beta_{D_2}$, or $\alpha_{D_2}\beta_{D_2}$, as expected from theory.

DISCUSSION

The aim of this study was to establish a quaternary model of the $\alpha_2\beta_2$ phenylalanyl-tRNA synthetase. The technique used is the measurement of the neutron scattering intensity at low angles and the determination of radii of gyration. Taking into account the specific deuteration of the α and β subunits in the tetramer and the variation of contrast, the extrapolated in situ R_G values of the α_2 and β_2 pairs could be obtained. These values, $51 \pm 2 \text{ \AA}$ and $39 \pm 2 \text{ \AA}$, respectively, for R_{G,α_2} and R_{G,β_2} can be combined with the R_G values of the α subunit and of the $\alpha_2\beta_2$ tetramer as well as with d (the distance between centers of mass of each pair), in order to discuss models.

A spherical model for a hydrated α subunit would lead to an R_G of $26 \pm 1 \text{ \AA}$, not compatible with the experimental value of $38.4 \pm 1.5 \text{ \AA}$. This value is better accounted for by a prolate ellipsoid of revolution ($45 \text{ \AA} \times 45 \text{ \AA} \times 160 \text{ \AA}$) and an axial ratio of 3.5. An alternative oblate ellipsoid would lead to unrealistic values.

Two models of α_2 dimers were examined. The first one consists of two ellipsoids touching each other with their major axes being parallel. This limiting model is rejected because

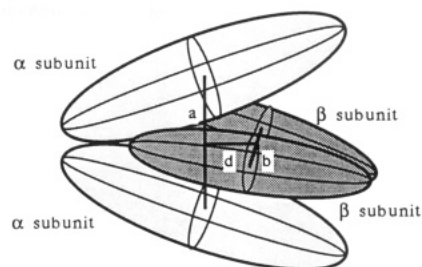


FIGURE 4: Model of the phenylalanyl-tRNA synthetase tetrameric structure derived from the experimental values. The $\alpha_2\beta_2$ tetrameric structure is characterized by (a) a distance of 67 \AA between the centers of mass of the two α promoters, (b) a distance of 45 \AA between the centers of mass of the two β promoters, and (d) a distance of 23 \AA between the centers of mass of the two α_2 and β_2 dimers. The main assumption of the model is closed contact between each element of the tetramer.

it leads to chord values greater than 210 \AA . This is incompatible with X-ray small-angle scattering measurements (unpublished data) indicating a maximum chord between 130 and 170 \AA for the $\alpha_2\beta_2$ tetramer and between 110 and 140 \AA for the isolated α subunit. For the second α_2 model, instead of being parallel, the major axes were allowed to make variable angles, with R_G values of α and α_2 maintained constant. With the constraint of the two ellipsoids being in contact and by use of the parallel axes theorem, best agreement is achieved with an angle of 38° between the axes. This implies a maximum chord of 160 \AA (the major axis of the α subunit in this case) and a distance of 67 \AA between the centers of mass of each α promoter. Noteworthy, the latter distance directly follows from the $R_{G,\alpha}$ and R_{G,α_2} experimental values, independently of the discussed model.

As mentioned earlier, the parameters for the β promoter could not be obtained, due to precipitation, but a hydrated equivalent sphere calculated from the M_r would have an R_G of 20 \AA . If these two spheres were in contact, the R_G value of the β_2 pair would be 32.5 \AA , incompatible with the in situ analysis ($R_{G,\beta_2} = 39 \pm 2 \text{ \AA}$). By imposing R_{G,β_2} and by assuming that the β_2 pair is composed of two tangent ellipsoids with their major axes being parallel, it is possible to calculate the R_G of each promoter and its axial ratio (36.4 \AA , $a/b = 5.6$). Under these conditions, the β_2 pair is elongated with a maximal chord of 158 \AA . Such a chord value is compatible with that of the tetramer enzyme, as deduced from the X-ray measurements. However, more globular shapes of the β promoter could be achieved with a variable angle between the major axes of the promoters. We have therefore assumed that the β subunits form an angle between their major axes, similarly to the case of the α_2 pair, and with an imposed d value. This leads to a unique solution for the parameters of the β_2 dimer, with an angle of 30° between axes, a promoter R_G value of 30.6 \AA , and an axial ratio of each ellipsoidal promoter of 4.2 ($31 \text{ \AA} \times 31 \text{ \AA} \times 130 \text{ \AA}$). This optimal solution, for a tetrameric model of two dimers in contact, corresponds to a maximal chord of 134 \AA for the β_2 pair and a distance of 45 \AA between the centers of mass of each β promoter (Figure 4). By comparison with the predicted chords of the $\alpha_2\beta_2$ tetramer, it can be deduced that the small β subunits of phenylalanyl-tRNA synthetase are partially buried in the enzyme.

This is to be compared to the case of tryptophan synthase from *E. coli*, another heterotetrameric enzyme composed of two α subunits ($M_r = 29K$) and two β subunits ($M_r = 86K$) (Yanofsky et al., 1981). A neutron scattering study, performed by Ibel et al. (1985), showed that within the $\alpha_2\beta_2$ complex the two α subunits are completely separated, being situated on opposite sides of the β_2 core. This was confirmed by the

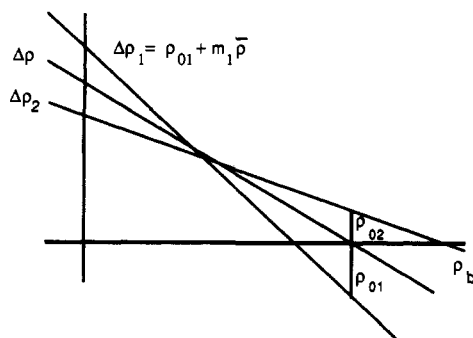


FIGURE 5: Schematic representation of the dependence of the excess scattering length densities of a particle ($\Delta\rho$) and of its constituents ($\Delta\rho_1, \Delta\rho_2$) on the solvent scattering length density (ρ_b).

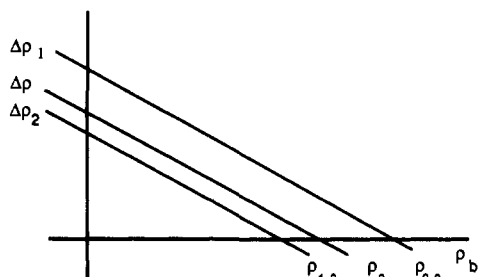


FIGURE 6: Dependence of the excess scattering length density of a particle ($\Delta\rho$) and of its constituents ($\Delta\rho_1, \Delta\rho_2$) on the solvent scattering length density (ρ_b) if $m_1 = m_2 = m$.

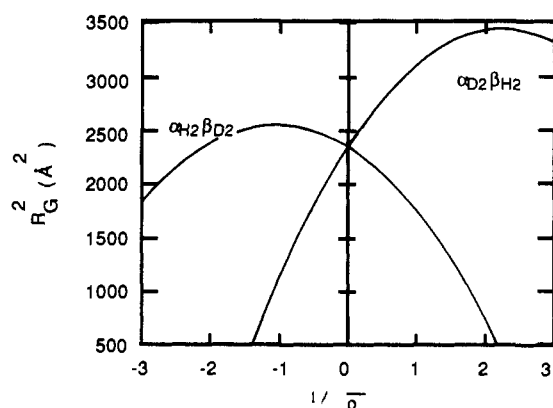


FIGURE 7: Stuhrmann plots (calculated) for particles composed of two copies of two components (α and β) with different volumes which are alternatively protonated (index H) or deuterated (index D).

crystallographic study of Hyde et al. (1988), which revealed that the four polypeptide chains are arranged nearly linearly in an $\alpha\beta\beta\alpha$ order forming a complex 150 Å long.

In the case of phenylalanyl-tRNA synthetase, we have already mentioned that, in the neutron experiments, the α promoters always showed identical Guinier plots, even at a concentration of 6 mg/mL. This indicates that an α_2 dimer does not form spontaneously. In contrast, isolated β subunits showed a strong tendency to aggregate, precluding the study of their hydrodynamical parameters. It is tempting therefore to propose that the small β_2 dimer serves as a core for inducing further association of the two larger α protomers in an $\alpha\beta\beta\alpha$ fashion. This building of the enzyme molecule would impose α/β interfaces and an α_2 geometry essential for sustaining both the activation of phenylalanine and the aminoacylation of tRNA. This idea is in agreement with affinity-labeling studies showing that the aminoacyl adenylate site would be created at the contact areas between the α and β subunits (Khodyreva et al., 1985) and that the tRNA binding site is mainly formed by the α polypeptide chain, provided it is engaged within the

native $\alpha_2\beta_2$ structure (Hountondji et al., 1987).

Recently, phenylalanyl-tRNA synthetase from *Thermus thermophilus* was crystallized (Chernaya et al., 1987). Hopefully, the determination of the X-ray structure of this enzyme, which is likely to be very similar to the *E. coli* one, will help to evaluate our present model and to discriminate between the various permitted organizations between the subunits.

Registry No. Phenylalanyl-tRNA synthetase, 9055-66-7.

REFERENCES

- Chernaya, M. M., Korolev, S. V., Reshatnikova, L. S., & Safra, M. G. (1987) *J. Mol. Biol.* 198, 555-556.
- Dessen, P., Blanquet, S., Zaccari, G., & Jacrot, B. (1978) *J. Mol. Biol.* 126, 293-313.
- Dessen, P., Fayat, G., Zaccari, G., & Blanquet, S. (1982) *J. Mol. Biol.* 154, 603-613.
- Dessen, P., Ducruix, A., Hountondji, C., May, R. P., & Blanquet, S. (1983a) *Biochemistry* 22, 281-284.
- Dessen, P., Zaccari, G., & Blanquet, S. (1983b) *Biochimie* 67, 637-641.
- Ducruix, A., Hounwanou, N., Reinbolt, J., Boulanger, Y., & Blanquet, S. (1983) *Biochim. Biophys. Acta* 741, 244-250.
- Fayat, G., Blanquet, S., Dessen, P., Batelier, G., & Waller, J. P. (1974) *Biochimie* 56, 35-41.
- Fayat, G., Fromant, M., Kalogerakos, T., & Blanquet, S. (1983a) *Biochimie* 65, 221-225.
- Fayat, G., Mayaux, J. F., Sacerdot, C., Fromant, M., Springer, M., Grunberg-Manago, M., & Blanquet, S. (1983b) *J. Mol. Biol.* 171, 239-261.
- Guinier, A., & Fournet, G. (1955) in *Small Angle Scattering of X Rays*, Wiley, New York.
- Hountondji, C., Schmitter, J. M., Beauvallet, C., & Blanquet, S. (1987) *Biochemistry* 26, 5433-5439.
- Hyde, C. C., Ahmed, S. A., Padlan, E. A., Miles, E. W., & Davies, D. L. (1988) *J. Biol. Chem.* 263, 17857-17871.
- Ibel, K. (1976) *J. Appl. Crystallogr.* 9, 630-643.
- Ibel, K., May, R. P., Kirschner, K., Lane, A. N., Szadkowski, H., Dauvergne, M. T., & Zulauf, M. (1985) *Eur. J. Biochem.* 151, 505-514.
- Jacrot, B. (1976) *Rep. Progr. Phys.* 39, 911-953.
- Jacrot, B., & Zaccari, G. (1981) *Biopolymers* 20, 2413-2426.
- Khodyreva, S. N., Moor, N. A., Aniklova, V. N., & Lavrik, O. I. (1985) *Biochim. Biophys. Acta* 830, 206-212.
- Koch, M. H. J., & Stuhrmann, H. B. (1979) *Methods Enzymol.* 59, 670-706.
- Lederer, H., May, R. P., Kjems, J. K., Schaefer, W., Crespi, H. L., & Heumann, H. (1986) *Eur. J. Biochem.* 156, 655-659.
- May, R. P., Ibel, K., & Haas, J. (1982) *J. Appl. Crystallogr.* 15, 15-19.
- Mechulam, Y., Fayat, G., & Blanquet, S. (1985) *J. Bacteriol.* 163, 787-791.
- Plumbridge, J. A., Springer, M., Goursot, G. M., & Grunberg-Manago, M. (1980) *Gene* 11, 38-42.
- Schimmel, P., & Söll, D. (1979) *Annu. Rev. Biochem.* 48, 601-648.
- Stöckel, P., May, R. P., Strell, I., Cejka, Z., Hoppe, W., Heumann, H., Zillig, W., Crespi, H. L., Katz, J. J., & Ibel, K. (1979) *J. Appl. Crystallogr.* 12, 176-185.
- Stöckel, P., May, R. P., Strell, I., Cejka, Z., Hoppe, W., Heumann, H., Zillig, W., & Crespi, H. L. (1980a) *Eur. J. Biochem.* 112, 411-417.
- Stöckel, P., May, R. P., Strell, I., Cejka, Z., Hoppe, W., Heumann, H., Zillig, W., & Crespi, H. L. (1980b) *Eur. J. Biochem.* 112, 419-427.

- Stuhrmann, H. B. (1974) *J. Appl. Crystallogr.* 7, 173–178.
 Timmins, P. A., & Zaccai, G. (1988) *Eur. Biophys. J.* 15, 257–268.
 Yanofsky, C., Platt, T., Crawford, I. P., Nichols, B. P., Christie, G. E., Horowitz, H., van Cleemput, M., & Wu, A. M. (1981) *Nucleic Acids Res.* 9, 6647–6668.
 Zaccai, G., & Jacrot, B. (1982) *Annu. Rev. Biophys. Bioeng.* 12, 139–157.

APPENDIX: CONSIDERATIONS ON STUHRMANN PLOTS OF PARTICLES WITH TWO CONSTITUENTS OF DIFFERENT SCATTERING LENGTH DENSITY

Koch and Stuhrmann (1978) have shown that for an inhomogeneous particle, composed essentially of two constituents (subunits) of different scattering length density, the distance of the centers of scattering mass d of the two constituents can be obtained from the β parameter in Stuhrmann's equation (Stuhrmann et al., 1975; Cotton & Benoit, 1975):

$$R^2 = R_c^2 + \alpha/\bar{\rho} - \beta/\bar{\rho}^2 \quad (\text{A1})$$

where R is the observed radius of gyration of the whole particle at a given (coherent) excess scattering length density (contrast) $\bar{\rho} = \rho_o - \rho_b$ and

$$\alpha = \int \rho_s(r)r^2 dr/V_c \quad (\text{A1a})$$

$$\beta = \left[\int \rho_s(r)r dr/V_c \right]^2 \quad (\text{A1b})$$

R_c is the radius of gyration of the particle at "infinite contrast", which is not necessarily the radius of gyration of a compact particle [cf. Witz (1983)], and $\rho_s(r)$ is the difference (fluctuation) between the scattering length density of the real particle $\rho(r)$ and ρ_o , the solvent scattering length (ρ_b) that matches the average scattering length density of the particle. With this definition

$$\int \rho_s(r) dr = 0 \quad (\text{A1c})$$

Even if solvent exchange is taken into account, an equation of the form of eq A1, with different definitions of α and β , still holds (Witz, 1983). R_c , α , β , and, consequently, d can be found by comparing eq A1 with another description of R , the parallel axes theorem of classical mechanics, applied to scattering (Damaschun et al., 1968):

$$R^2 = c_1 R_1^2 + c_2 R_2^2 + c_1 c_2 d^2 \quad (\text{A2})$$

where

$$c_i = \Delta\rho_i V_i / (\Delta\rho_1 V_1 + \Delta\rho_2 V_2) \quad (\text{A2a})$$

is the reduced scattering mass, V_i is the volume, $\Delta\rho_i$ is the excess scattering length density, and R_i is the radius of gyration of constituent i , $i = 1$ or 2 .

Moore (1981) has used a similar formalism for judging the quality of the estimation of the R_G of a single (very) small component within a macromolecular assembly like a ribosomal subunit. In our treatment, we are interested in the influence of the scattering contributions from two constituents of different, but similar, size on the R_G of their complex as a function of the scattering contrast.

In order to avoid the problem of treating solvent exchange phenomena in detail, let V , V_1 , and V_2 be large enough to circumscribe the respective particles, so that we can assume that only the scattering length densities, but not the volumes, vary with the contrast. Evidently

$$c_1 + c_2 = 1 \quad (\text{A2b})$$

$$\Delta\rho_1 V_1 + \Delta\rho_2 V_2 = \Delta\rho V \quad (\text{A2c})$$

hold with $V = V_1 + V_2$. With the notations

$$f_i = V_i/V \quad (\text{A3a})$$

$$f_1 + f_2 = 1 \quad (\text{A3b})$$

$$\Delta\rho_i = \rho_{oi} + m_i \bar{\rho} \quad i = 1 \text{ or } 2 \quad (\text{A3c})$$

where $\Delta\rho_i$ is the excess scattering length density of constituent i at the match point of the whole particle and m_i is the slope of $\Delta\rho_i$, m_i is about -1 : $m_i = -1$ in the case of no exchange (Figure 5).

Similarly, we can write

$$\Delta\rho = \rho - \rho_b = m \bar{\rho} \quad (\text{A3d})$$

where $\bar{\rho}$ is the average scattering length density of the particle, which itself may depend on the solvent composition, e.g., because of H/D exchange. Of course, $\Delta\rho = 0$ at the match point. Since

$$\begin{aligned} \Delta\rho &= \Delta\rho_1 f_1 + \Delta\rho_2 f_2 \\ &= f_1 \rho_{o1} + f_2 \rho_{o2} + (m_1 f_1 + m_2 f_2) \bar{\rho} \end{aligned} \quad (\text{A3e})$$

we find that

$$f_1 \rho_{o1} + f_2 \rho_{o2} = 0 \quad (\text{A4a})$$

$$m = m_1 f_1 + m_2 f_2 \quad (\text{A4b})$$

$$c_i = f_i(\rho_{oi} + m_i \bar{\rho})/m \bar{\rho} \quad (\text{A4c})$$

Using eq A4c in eq A2, we get

$$\begin{aligned} R^2 &= f_1 \rho_{o1} R_1^2 / m \bar{\rho} + f_2 \rho_{o2} R_2^2 / m \bar{\rho} + f_1 m_1 R_1^2 / m + \\ &\quad f_2 m_2 R_2^2 / m + \\ &\quad f_1 f_2 d^2 (\rho_{o1} \rho_{o2} + m_1 \bar{\rho} \rho_{o2} + m_2 \bar{\rho} \rho_{o1} + m_1 m_2 \bar{\rho}^2) / \bar{\rho}^2 \end{aligned} \quad (\text{A5})$$

which finally results in

$$\begin{aligned} R_c^2 &= (f_1 m_1 / m) R_1^2 + (f_2 m_2 / m) R_2^2 + (f_1 f_2 m_1 m_2 / m^2) d^2 \\ \alpha &= (f_1 \rho_{o1} / m) R_1^2 + (f_2 \rho_{o2} / m) R_2^2 + \\ &\quad [f_1 f_2 (m_1 \rho_{o2} + m_2 \rho_{o1}) / m^2] d^2 \quad (\text{A6}) \\ \beta &= -(f_1 f_2 \rho_{o1} \rho_{o2} / m^2) d^2 \end{aligned}$$

Here we assume that the radii of gyration of the constituents and d itself do not depend on $\bar{\rho}$. In the case of d this necessitates that the exchange in both constituents takes place without changing their centers of scattering masses, i.e., symmetrically, but not necessarily homogeneously. Evidently, the set of eqs A6 is quite complicated to evaluate. It is useful to look at two special cases:

(1) The two constituents have the same match points:

$$\rho_{o1} = \rho_{o2} = 0$$

Interestingly, in this case, $\alpha = 0$ and $\beta = 0$, even if the exchange behavior is different for both constituents.

(2) The slopes of $\Delta\rho_1$ and $\Delta\rho_2$ are identical (Figure 6):

$$m_1 = m_2 = m \text{ (according to eq A4b)}$$

It follows that

$$\begin{aligned} R_c^2 &= f_1 R_1^2 + f_2 R_2^2 + f_1 f_2 d^2 \text{ (Stuhrmann et al., 1978)} \\ \alpha &= (f_1 \rho_{o1} / m) R_1^2 + (f_2 \rho_{o2} / m) R_2^2 + [f_1 f_2 (\rho_{o1} + \rho_{o2}) / m] d^2 \end{aligned} \quad (\text{A7})$$

$$\beta = -(f_1 f_2 \rho_{o1} \rho_{o2} / m^2) d^2$$

Defining $\rho_{i,o}$ as the match point of constituent i and taking into account

$$\rho_{oi} = m(\rho_o - \rho_{i,o}) \quad (\text{A8})$$

we find, with eqs A3b and A4a

$$\begin{aligned} \rho_{1,o} - \rho_{2,o} &= (\rho_{o2} - \rho_{o1}) / m \\ &= \rho_{o2} / f_1 m = -\rho_{o1} / f_2 m \end{aligned} \quad (\text{A9})$$

or

$$\rho_{o1} = -f_2 m(\rho_{1,o} - \rho_{2,o}) \quad (\text{A9a})$$

$$\rho_{o2} = f_1 m(\rho_{1,o} - \rho_{2,o}) \quad (\text{A9b})$$

Introducing this into eq A7, we finally get

$$\alpha = -f_1 f_2 (\rho_{1,o} - \rho_{2,o}) [R_1^2 - R_2^2 - (f_1 - f_2) d^2] \quad (\text{A10})$$

$$\beta = f_1^2 f_2^2 (\rho_{1,o} - \rho_{2,o})^2 d^2$$

This is in disagreement with the corresponding formula for β by Koch and Stuhmann (1978), which also lacks the volume fractions.

In the case of an exactly symmetrical exchange of particles 1 and 2, i.e., $\rho_{1,o} = \rho_{2,o}$ and $\rho_{2,o} = \rho_{1,o}$, β remains unchanged and α changes its sign, but not its values, leading to Stuhmann plots (R^2 vs $1/\bar{p}$) which are symmetrical with respect to the $1/\bar{p}$ axis. If, however, this symmetry is not fulfilled, e.g., because the level of deuteration of constituent 1 is not the same as that of constituent 2, α and β are different for the pairs H_1D_2 and D_1H_2 .

If the constituents are of unequal size, the Stuhmann plot of one of these pairs can be shifted sufficiently far away from the origin of $1/\bar{p}$ that the curvature of the parabola cannot

be observed due to the errors of the radius of gyration determinations at low contrasts, i.e., large $1/\bar{p}$ values (Figure 7). It is important to note that inhomogeneity of one of the constituents is *not* required for explaining this fact (although it might be easier to use this explanation for chemical reasons).

ACKNOWLEDGMENTS

We express our gratitude to H. Lederer for useful discussions.

REFERENCES

- Cotton, J. P., & Benoit, H. (1975) *J. Phys.* 36, 905–910.
- Damaschun, G., Fichtner, P., Pürschel, H. V., & Reich, J. G. (1968) *Acta Biol. Med. Ger.* 21, 309–316.
- Koch, M. H. J., & Stuhmann, H. B. (1979) *Methods Enzymol.* 59, 670–706.
- Moore, P. B. (1981) *J. Appl. Crystallogr.* 14, 237–240.
- Stuhmann, H. B., Tardieu, A., Mateu, L., Sardet, C., Luzzati, V., Aggerbeck, L., & Scanu, A. M. (1975) *Proc. Natl. Acad. Sci. U.S.A.* 72, 2270–2273.
- Stuhmann, H. B., Koch, M. H. J., Parfait, R., Haas, J., Ibel, K., & Crichton, R. R. (1978) *J. Mol. Biol.* 119, 203–212.
- Witz, J. (1983) *Acta Crystallogr.* A39, 706–711.

On the Mechanism of Transbilayer Transport of Phosphatidylglycerol in Response to Transmembrane pH Gradients[†]

T. E. Redelmeier,[†] M. J. Hope,^{†,§} and P. R. Cullis^{*,†,§}

Department of Biochemistry, The University of British Columbia, Vancouver, British Columbia, Canada V6T 1W5, and The Canadian Liposome Company Ltd., Suite 308, 267 Esplanade, North Vancouver, Canada V7M 1A5

Received July 24, 1989; Revised Manuscript Received November 8, 1989

ABSTRACT: Previous work [Hope et al. (1989) *Biochemistry* 28, 4181–4187] has shown that asymmetric transmembrane distributions of phosphatidylglycerol (PG) in PG–phosphatidylcholine (PC) large unilamellar vesicles can be induced in response to transbilayer pH gradients (ΔpH). Here the mechanism of PG transport has been investigated. It is shown that PG movement in response to ΔpH is consistent with permeation of the uncharged (protonated) form and that the half-time for transbilayer movement of the uncharged form can be on the order of seconds at 45 °C. This can result in rapid pH-dependent transmembrane redistributions of PG. The rate constant for transbilayer movement exhibits a large activation energy (31 kcal/mol) consistent with transport of neutral dehydrated PG where dehydration of the (protonated) phosphate presents the largest barrier to transmembrane diffusion. It is shown that acyl chain saturation, chain length, and the presence of cholesterol modulate the rate constants for PG transport in a manner similar to that observed for small nonelectrolytes.

Phospholipids in biological membranes frequently exhibit asymmetric transbilayer distributions. This has been shown for the erythrocyte plasma membrane (Op den Kamp, 1979), the platelet plasma membrane (Chap et al., 1977), the rat liver endoplasmic reticulum (Higgins & Pigott, 1982; Sleight & Pagano, 1985), the Golgi complex (van Meer et al., 1987), and the inner mitochondrial membrane (Krebs et al., 1978). Two general findings have been made. First, in the plasma membrane of the erythrocyte, lymphocyte, or platelet, the

amino-containing phospholipids phosphatidylserine and phosphatidylethanolamine are primarily located in the inner (cytoplasmic) monolayer (IM)¹ whereas the choline-containing lipids phosphatidylcholine (PC) and sphingomyelin are located in the outer monolayer (OM). Second, the transbilayer

[†] This research was supported by the Medical Research Council of Canada (MRC). P.R.C. is a MRC Scientist.

^{*} To whom correspondence should be addressed at the Department of Biochemistry, The University of British Columbia.

[†] The University of British Columbia.

[§] The Canadian Liposome Company Ltd.

¹ Abbreviations: BSA, bovine serum albumin; Chol, cholesterol; DOPC, dioleoylphosphatidylcholine; DOPG, dioleoylphosphatidylglycerol; DPOPC, dipalmitoleoylphosphatidylcholine; DPPC, dipalmitoylphosphatidylcholine; EPC, egg phosphatidylcholine; EPG, egg phosphatidylglycerol; EPPS, *N*-(2-hydroxyethyl)piperazine-*N'*-3-propanesulfonic acid; HEPES, *N*-(2-hydroxyethyl)piperazine-*N'*-2-ethanesulfonic acid; IM, inner monolayer; LPC, lysophosphatidylcholine; LUVs, large unilamellar vesicles; MES, 2-(*N*-morpholino)ethanesulfonic acid; MOPG, monooleoylphosphatidylglycerol; OM, outer monolayer; PA, phosphatidic acid; PG, phosphatidylglycerol; PIPES, piperazine-*N*,*N'*-bis(2-ethanesulfonic acid); PS, phosphatidylserine; SA, stearylamine.